Influence of ϕ mesons on negative kaons in Ni + Ni collisions at 1.91A GeV beam energy

K. Piasecki,[1,*] N. Herrmann,[2] R. Averbeck,[3] A. Andronic,[3] V. Barret,[4] Z. Basrak,[5] N. Bastid,[4] M. L. Benabderrahmane,[2] M. Berger,[6,7] P. Buehler,[8] M. Cargnelli,[8] R. Čaplar,[5] P. Crochet,[4] O. Czerwiakowa,[1] I. Deppner,[2] P. Dupieux,[4] M. Dželalija,[9] L. Fabbietti,[6,7] Z. Fodor,[10] P. Gasik,[1,6] I. Gašparić,[5] Y. Grishkin,[11] O. N. Hartmann,[3] K. D. Hildenbrand,[3] B. Hong,[12] T. I. Kang,[3,12] J. Kecskemeti,[10] Y. J. Kim,[3] M. Kirejczyk,[1] M. Kiš,[3,5] P. Koczon,[3] R. Kotte,[13] A. Lebedev,[11] Y. Leifels,[3] A. Le Fèvre,[3] J. L. Liu,[2,14] X. Lopez,[4] V. Manko,[15] J. Marton,[8] T. Matulewicz,[1] R. Münzer,[6,7] M. Petrovici,[16] F. Rami,[17] A. Reischl,[2] W. Reisdorf,[3] M. S. Ryu,[12] P. Schmidt,[8] A. Schüttauf,[3] Z. Seres,[10] B. Sikora,[1] K. S. Sim,[12] V. Simion,[16] K. Siwek-Wilczyńska,[1] V. Smolyankin,[11] K. Suzuki,[8] Z. Tymiński,[1] P. Wagner,[17] I. Weber,[9] E. Widmann,[8] K. Wiśniewski,[1,2] Z. G. Xiao,[18] I. Yushmanov,[15] Y. Zhang,[2,19] A. Zhilin,[11] V. Zinyuk,[2] and J. Zmeskal[8]

(FOPI Collaboration)

[1]*Institute of Experimental Physics, Faculty of Physics, University of Warsaw, Warsaw, Poland*

[2]*Physikalisches Institut der Universität Heidelberg, Heidelberg, Germany*

[3]*GSI Helmholtzzentrum für Schwerionenforschung GmbH, Darmstadt, Germany*

[4]*Laboratoire de Physique Corpusculaire, IN2P3/CNRS, and Université Blaise Pascal, Clermont-Ferrand, France*

[5]*Ruđer Bošković Institute, Zagreb, Croatia*

[6]*Excellence Cluster Universe, Technische Universität München, Garching, Germany*

[7]*E12, Physik Department, Technische Universität München, Garching, Germany*

[8]*Stefan-Meyer-Institut für subatomare Physik, Österreichische Akademie der Wissenschaften, Wien, Austria*

[9]*University of Split, Split, Croatia*

[10]*Wigner RCP, RMKI, Budapest, Hungary*

[11]*Institute for Theoretical and Experimental Physics, Moscow, Russia*

[12]*Korea University, Seoul, Korea*

[13]*Institut für Strahlenphysik, Helmholtz-Zentrum Dresden-Rossendorf, Dresden, Germany*

[14]*Harbin Institute of Technology, Harbin, China*

[15]*National Research Centre "Kurchatov Institute", Moscow, Russia*

[16]*Institute for Nuclear Physics and Engineering, Bucharest, Romania*

[17]*Institut Pluridisciplinaire Hubert Curien and Université de Strasbourg, Strasbourg, France*

[18]*Department of Physics, Tsinghua University, Beijing 100084, China*

[19]*Institute of Modern Physics, Chinese Academy of Sciences, Lanzhou, China*

(Received 13 December 2014; revised manuscript received 10 March 2015; published 13 May 2015)

ϕ and K^- mesons from Ni+Ni collisions at the beam energy of 1.91A GeV have been measured by the FOPI spectrometer, with a trigger selecting central and semicentral events amounting to 52% of the total cross section. The phase-space distributions, and the total yield of K^-, as well as the kinetic energy distribution and the total yield of ϕ mesons are presented. The ϕ/K^- ratio is found to be $0.44 \pm 0.07(\text{stat})^{+0.16}_{-0.10}(\text{syst})$, meaning that about 22% of K^- mesons originate from the decays of ϕ mesons, occurring mostly in vacuum. The inverse slopes of direct kaons are up to about 15 MeV larger than the ones extracted within the one-source model, signaling that a considerable share of gap between the slopes of K^+ and K^- could be explained by the contribution of ϕ mesons to negative kaons.

DOI: 10.1103/PhysRevC.91.054904 PACS number(s): 25.75.Dw, 13.60.Le

I. INTRODUCTION

Nucleus-nucleus collisions at the beam kinetic energies of 1–2A GeV offer the unique possibility to study the onset of the strangeness production. The emergence of strangeness at beam energies below the thresholds in free nucleon-nucleon (NN) collisions is facilitated by the appearance of resonances and mesons in the heated ($T \approx 100$ MeV) and compressed (2–3 times above the normal nuclear density ρ_0) collision zone, where the basic properties of particles like effective mass and decay constant are modified [1–7].

The knowledge about the emission yields and kinematical properties of ϕ mesons produced in nucleus-nucleus collisions is very limited at the beam energy below 10A GeV as the experimental data is scarce in this beam energy region [8–11]. Possible channels of in-medium ϕ meson production include $BB \to BB\phi, MB \to N\phi, \rho\pi \to \phi$ ($B = [N, \Delta], M = [\rho, \pi]$).

Calculations within the BUU transport model for the central Ni+Ni collisions at the beam energy of 1.93A GeV favor the dominance of the MB channels [12]. This system was measured in a previous work by the FOPI Collaboration, but the statistics (23 ± 7 events attributed to ϕ mesons) were insufficient for a quantitative comparison with the calculations [8].

Since the mean decay path of ϕ is 46 fm, most of these particles decay outside the collision zone. As its dominant decay channel is $\phi \to K^+K^-$ ($BR = 48.9\%$) [15], and the

*krzysztof.piasecki@fuw.edu.pl

freeze-out yields of ϕ and K^- are found to be of comparable order [8–10], ϕ decays are the source of K^- mesons that are mostly unaffected by presence of the surrounding medium, in contrast to those negative kaons produced directly in the collision zone. Therefore, evaluation of the $\phi/\ K^-$ ratio is of importance for the studies of the modifications of K^- properties in medium. In the discussed energy range this ratio was reported for the Ar+KCl collisions at 1.756A GeV [9].

In this paper we present the yield and kinetic energy distribution of ϕ, as well as the $\phi/\ K^-$ ratio for the collisions of Ni+Ni at the beam kinetic energy of 1.91A GeV, covering the most central 52% of the geometrical cross section.

II. EXPERIMENT

The experiment was carried out with the FOPI spectrometer, installed at the heavy-ion synchrotron SIS-18 at GSI, Darmstadt. The innermost detector is the azimuthally symmetric central drift chamber (CDC), covering the wide range of polar angles ($27^\circ < \theta_{\rm lab} < 113^\circ$). CDC is surrounded by two detectors in the barrel geometry, dedicated for the time-of-flight (ToF) measurements: multistrip multigap resistive plate counter [13], spanning $30^\circ < \theta_{\rm lab} < 53^\circ$, and the plastic scintillation barrel (PSB), covering $55^\circ < \theta_{\rm lab} < 110^\circ$. These devices are encircled by the magnet solenoid, delivering the magnetic field of $B = 0.617$T, and covered at front by the plastic scintillation wall (PSW). More details on characteristics and performance of the FOPI apparatus can be found in Ref. [14].

The ^{58}Ni ions, accelerated to the kinetic energy of 1.91A GeV, were incident on the 405 μm-thick ^{58}Ni target (corresponding to 1% interaction probability). By requiring the multiplicities of charged hits in PSW (PSB) to be $\geqslant 5$ ($\geqslant 1$), the trigger selected the sample of 7.6×10^7 central and semicentral events amounting to (52.0 ± 1.5)% of the total geometrical cross section. Assuming the simple geometrical model of interpenetrating spheres, and the sharp cut-off approximation between the maximum impact parameter and the total reaction cross section, the mean number of participant nucleons averaged over the impact parameter was estimated to be $\langle A_{\rm part}\rangle_{\rm b} = 49 \pm 1$.

III. DATA ANALYSIS

Particles traversing the CDC detector activate sense wires along their flight path, leaving series of hits, which are combined into tracks by the off-line procedure. While hitting the MMRPC (PSB) detector, particles activate one or a few neighboring strips, merged off line into hits. Subsequently, tracks in the CDC and hits in the ToF detectors are matched. A collection of tracks is used to calculate the position $\vec{v}$ of the event vertex. To reject the collisions occurred outside the target, a cut was applied on the component of the vertex position in the beam direction: $|v_z| < 15$ cm.

In order to select a sample of good-quality tracks, a set of cuts was applied. To suppress the contribution from the discontinuous tracks, the track was required to be constructed of at least 36 (32) hits for K^- (K^+). The asymmetry in the number of hits is due to the nonradial profile of sense wires of the CDC, so the negative particles generate more hits on average than the positive ones. As both charged kaons are produced in the target, two more conditions were imposed on transverse and longitudinal distance of closest approach between the track and the collision vertex: $|d_0| < 1.5$ cm and $|z_0| < 30$ cm, accordingly. Particles with the absolute values of charge higher than the elementary charge were rejected. Since some anisotropy was found in the azimuthal distribution of tracks in the backward zone of the CDC, the region of $\theta_{\rm lab} > 90^\circ$ was excluded from the analysis. The requirement of CDC-ToF matching imposes a lower limit on the transverse momentum of a particle spiralling in the magnetic field: $p_{\rm t} \geqslant 0.1$ GeV/c. To ensure the good matching between the track in the CDC device and the hit in a ToF detector, two additional conditions were imposed on the azimuthal and longitudinal distance between the extrapolation of the CDC track to the relevant ToF module, and the hit therein: $|\Delta\varphi| < 1.5^\circ$, $|\Delta z| < 30$ cm for the PSB, and $|\Delta\varphi| < 0.6^\circ$, $|\Delta z| < 25$ cm for the MMRPC.

Charged particle identification based on information from the CDC and ToF detectors is performed by tracing the correlation between momentum and velocity of a particle, as shown in Fig. 1. Events on this plane can be projected onto the mass parameter, using the relativistic formula $p = m\gamma v$. The capability to identify the charged kaons, limited to modest momenta for the PSB, has been largely enhanced in the MMRPC, due to the excellent timing performance and better granularity of the latter [13].

A. Negative kaons

For the analysis of K^-, the observation of signal and background ratio prompted to impose the high $p_{\rm t}$ limits of 0.57 GeV/c (MMRPC) and 0.35 GeV/c (PSB). To reconstruct the phase-space population of K^-, the experimental mass distribution was analyzed for every $p_{\rm t}$-$y_{\rm lab}$ cell, where $y_{\rm lab}$ denotes rapidity in the laboratory frame. The kaonic signal in this distribution was separated from the background composed of π^- mesons. A total of 9870 negative kaons were found in the CDC-ToF acceptance region. Influences of the choice of the binning of $p_{\rm t}$, $y_{\rm lab}$ and mass histograms, and of the choice of the minimum number of hits in a CDC track on the spectra presented in this paper were included in the relevant systematic errors.

B. ϕ mesons

For the reconstruction of the ϕ meson via the K^+K^- decay, the maximum momentum of K^+ (K^-) was set to 1.2 (0.85) GeV/c for the tracks matched with the MMRPC, and 0.72 (0.60) GeV/c for the PSB. Unequal selection of maximum momenta for K mesons of opposite charges is due to different signal strength, as seen in Fig. 1. To minimize the side effects on the edges of ToF detectors, the observation region of the ϕ meson phase space was trimmed to $95^\circ < \theta_{\rm NN} < 150^\circ$, where $\theta_{\rm NN}$ is the polar emission angle in the nucleon-nucleon center of mass frame.

The ϕ mesons were identified via the invariant mass analysis of K^+K^- pairs (see Fig. 2), a dominant ϕ meson decay channel. The uncorrelated background was obtained with the mixed events method and normalized to the true pair distribution in the region $1.05 < M_{\rm inv} < 1.18$ GeV/c^2. After subtraction of the background, about 170 ϕ mesons were found

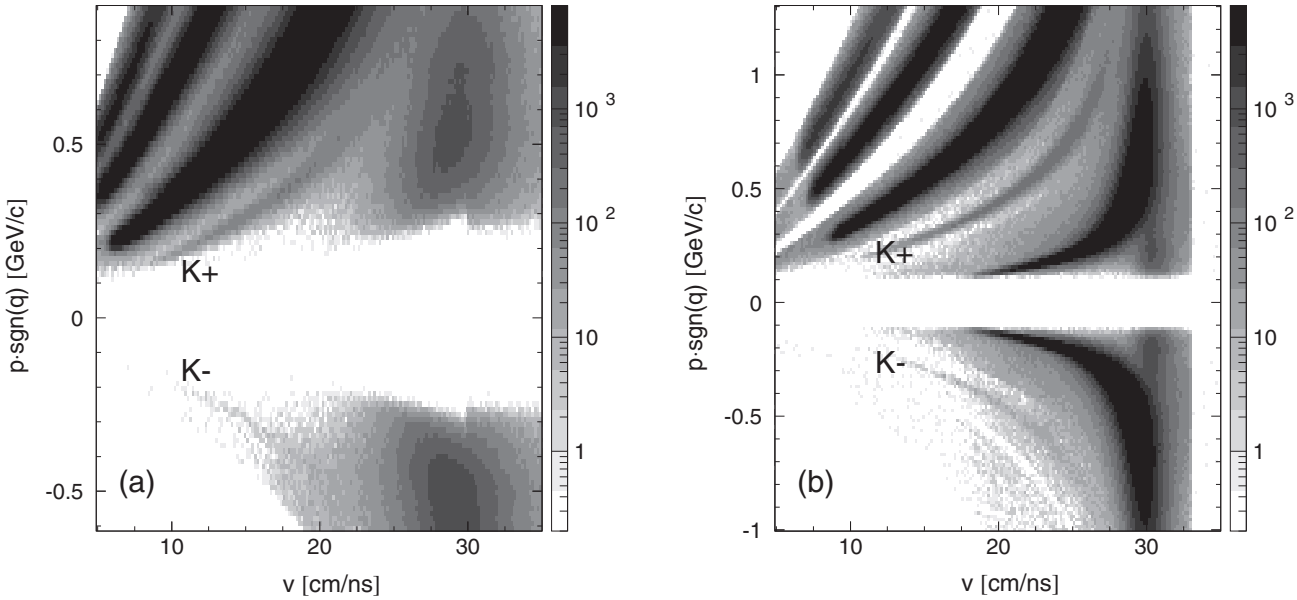

FIG. 1. Particle identification based on relativistic momentum-velocity dependence, with (a) PSB, and (b) MMRPC detectors.

under the peak. Within the range of ±2 standard deviations of the fitted Gaussian distribution the signal to background ratio was found to be 1.1, and significance 9.3. The values of cut parameters leading to the identification of ϕ mesons were further varied, and the propagation of these changes on the results were included in their systematic uncertainties.

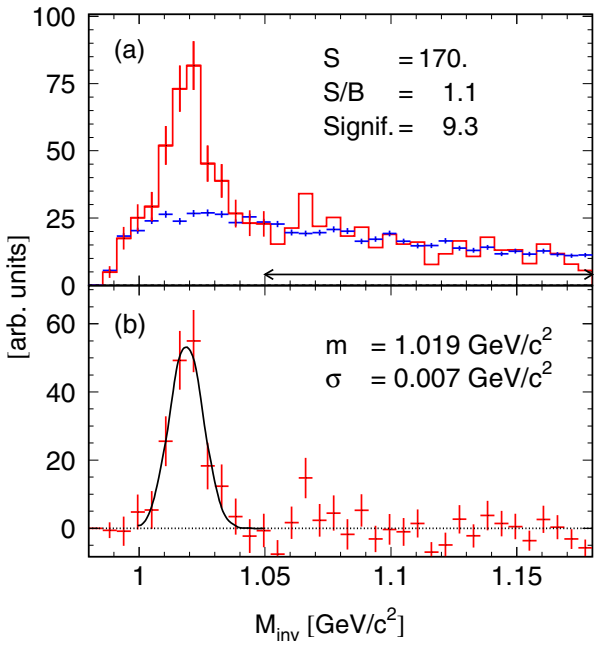

FIG. 2. (Color online) (a) Invariant mass plot of (solid line) true, and (scattered points) mixed K^+K^- pairs. (b) ϕ meson signal obtained after background subtraction.

IV. EFFICIENCY EVALUATION

A. Standard efficiency correction

1. Negative kaons

The GEANT [16] package for detector simulation was employed to obtain the efficiency correction. Negative kaons were generated according to the homogeneous p_t-y_{lab} distribution, and added to the events of the Ni+Ni collisions at the beam energy of 1.91A GeV, simulated by the IQMD code [17]. For both K^- and ϕ mesons, the simulated events were treated using the same off-line analysis package, as for the experimental data. The efficiency distribution of K^- for the regions of phase space covered by MMRPC and PSB detectors is shown in Fig. 3(a). For the momenta higher than 0.5 GeV/c it reaches about 50%. A drop of efficiency at lower p_t is caused by the higher probability for the kaon to decay on its path to either of two ToF detectors.

2. ϕ mesons

For the efficiency evaluation, the mass of the ϕ mesons was sampled from the Breit-Wigner distribution, and the phase space was populated by pulling from the Boltzmann distribution scaled by the anisotropy term

$$\frac{d^2N}{dEd\vartheta} \sim pE\exp(-E/T_s)(1+\alpha\cos^2\vartheta), \qquad (1)$$

where T_s is the temperature of the source, and α is the anisotropy parameter. Sampled mesons were subsequently boosted to the laboratory frame. The parameters in Eq. (1) were varied in the range of $T_s \in [80, 130]$ MeV, $\alpha \in [0.0, 1.0]$, as roughly expected from the systematics for other strange particles produced in this beam energy range and collision centrality [6]. Differences of the obtained efficiency corrections due to variations of these parameters were further included in the systematic uncertainties of the investigated physics

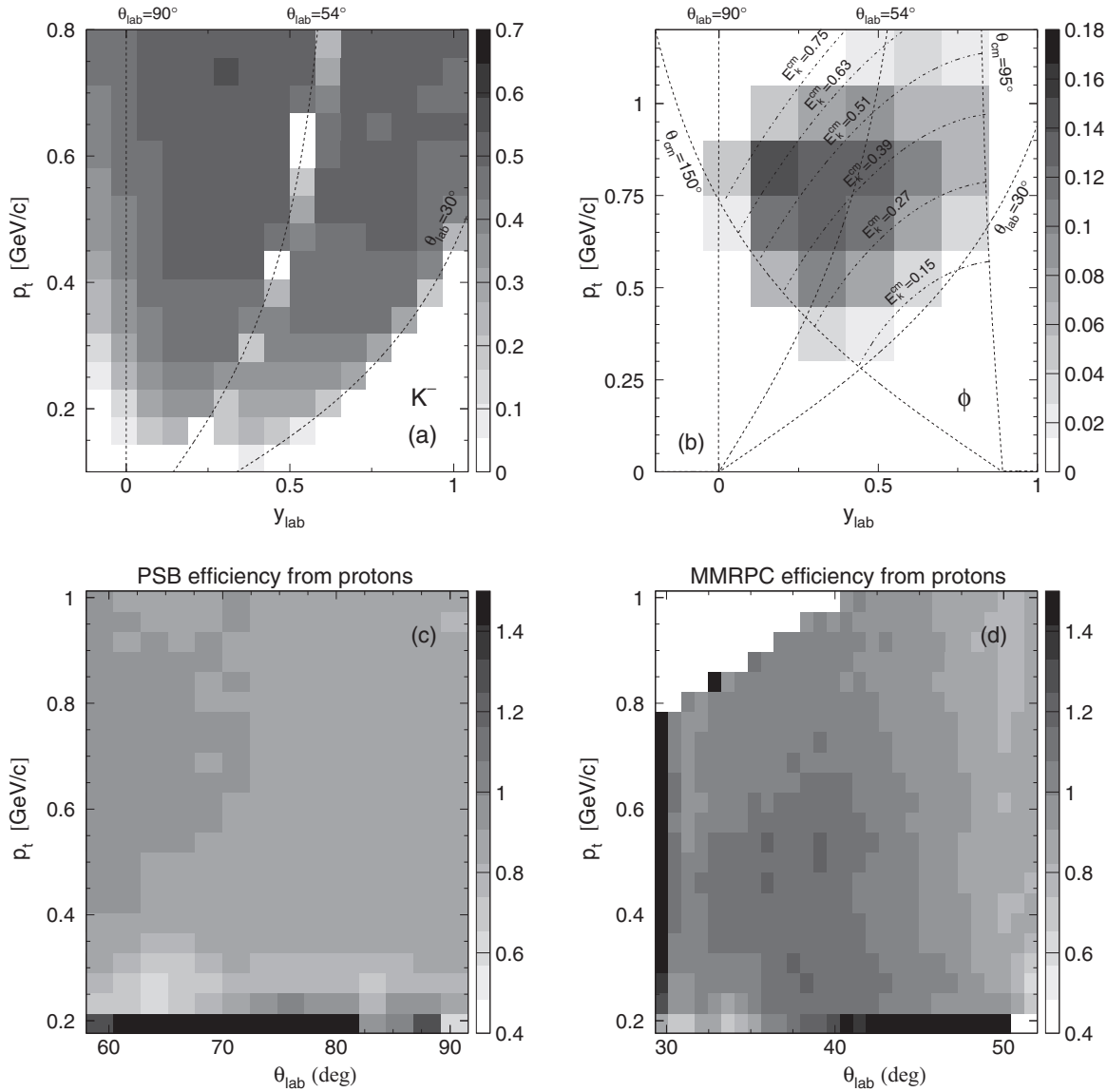

FIG. 3. Top row: efficiency distribution for (a) K^-, and (b) ϕ mesons (at $T_s = 100$ MeV, $\alpha = 0$). Bottom row: maps of internal efficiency of (c) PSB, and (d) MMRPC detectors, obtained with protons. See text for details.

variables, as discussed below. ϕ mesons were subsequently embedded in the Ni+Ni collisions, simulated with the IQMD code. Figure 3(b) shows the phase-space efficiency distribution for $T_s = 100$ MeV, and $\alpha = 0$. As the ϕ mesons have been analysed both inclusively and by studying the kinetic energy distribution, the appropriate efficiencies were obtained for either case separately.

B. Internal efficiency of ToF detectors

Following the reported inhomogeneity in the longitudinal position response of the MMRPC detector, shown in Fig. 12 of Ref. [13], the phenomenological study of the internal efficiency of this detector was performed. While the effects of geometry and matching are the regular part of the GEANT-based efficiency determination procedure, possible internal MMRPC inefficiencies were not included so far. This additional efficiency factor was pursued by constructing first the ratio of CDC tracks with associated hit in a ToF (MMRPC, PSB) detector to all the reconstructed CDC tracks. This ratio was obtained independently for the experimental and simulated data. Next both results were divided to yield the internal efficiency factor ε^{ToF}, according to:

$$\varepsilon^{ToF}(\vartheta, p_t) = \frac{N^{\mathrm{ToF}}_{\mathrm{exp}}}{N^{\mathrm{CDC}}_{\mathrm{exp}}} \Big/ \frac{N^{\mathrm{ToF}}_{\mathrm{sim}}}{N^{\mathrm{CDC}}_{\mathrm{sim}}}, \tag{2}$$

where ToF $\in$ {MMRPC, PSB}. The resulting $\varepsilon(\vartheta, p_t)$ maps for both PSB and MMRPC detectors are shown in Fig. 3. Particularly noticeable is the heap structure around the center of the MMRPC detector ($\vartheta \approx 38^\circ$), reported also in Ref. [13]. A correction of the distributions of K mesons was done on an event-by-event basis by weighting every kaon event with the factor $1/\varepsilon^{ToF}(\vartheta, p_t)$. In order to minimize the possible sensitivity of ε^{ToF} to particle's charge, corrections for negatively

charged kaons were performed using the map obtained from π^- mesons. Differences between maps obtained from protons, and π^- were found to be small (in the order of 5–7 %) and were manifested mainly in the global normalization.

V. RESULTS

A. Negative kaons

The transverse momentum spectra for consecutive slices of rapidity within the $0.34 < y_{\rm lab} < 0.89$ range, covered by the MMRPC, are shown in Fig. 4(a). They were fitted according to the Boltzmann-like function:

$$\frac{d^2N}{dp_t dy_{\rm NN}} = N p_t E \exp(-m_T/T_B), \tag{3}$$

where $m_T = \sqrt{p_T^2+m^2}$ is the transverse mass, and for every slice $y_{\rm NN}$ denotes the average value of rapidity in the NN frame, N is the normalization factor, and T_B is the inverse slope (also called the apparent temperature). The p_t spectra measured in the PSB region ($0 < y_{\rm lab} < 0.3$) had too poor statistics for the two-parameter fitting. Therefore, the normalization parameters were extracted only, by fitting the formula (3) with one of two fixed values of T_B: 45 and 60 MeV (differences in the results were accounted for in the evaluation of the systematic errors). The points of the rapidity distribution were obtained by an analytic integration of the formula (3) from 0 to ∞ for every slice,

$$\frac{dN}{dy_{\rm NN}} = N\cosh(y_{\rm NN})T_B^3\left(\frac{m^2}{T_B^2}+2\frac{m}{T_B}+2\right)\exp\left(-\frac{m}{T_B}\right), \tag{4}$$

where m is the particle's mass, and substituting the parameters obtained in the fit above. The obtained distribution is shown in Fig. 4(b). Note, that the N and T_B fit parameters are strongly anticorrelated. This anticorrelation was included in the error evaluation of the rapidity distribution. The magenta boxes on the above-mentioned plot correspond to the systematic errors arising from variations of all the applied cuts and binnings, except for the contribution from the choice of binning of the rapidity axis. Benefitting from the symmetry of the colliding system, the measured data points were reflected with respect to the midrapidity ($y_{\rm NN}^{\rm CM} = 0.89$), which allowed for a wide coverage of the K^- rapidity spectrum.

In order to obtain the K^- yield, the tails of the rapidity distribution were extrapolated. To assess the systematic error of this procedure, the data was fitted using two functions: the Gaussian and the linear one. Each of these functions was fitted in two ranges: $y_{\rm lab} < 0.3$, and 0.5. Of four possibilities, the variant resulting in the largest (smallest) reconstructed yield is shown as dashed (dotted) line in Fig. 4(b). The total yield of K^- was found to be:

$$P(K^-) = [9.84 \pm 0.21({\rm stat})^{+0.63}_{-0.57}({\rm syst})] \times 10^{-4} \tag{5}$$

per triggered event, where the systematic errors are given at the 95% confidence level. The measured part of the K^- yield amounts to 22% of the total. However, the relatively wide range of momenta and rapidity covered, and the symmetry of the colliding system allowed to minimize the assumptions on the overall shape profile of the rapidity distribution, and in consequence on the total yield of K^-.

B. ϕ mesons

The sample of ϕ mesons counts about 170 events. This number of events does not permit for a full-fledged analysis of its phase space, and thus for the reconstruction of the yield in a model-independent fashion. As a first step the yield was reconstructed directly by dividing the total number of events within the phase-space region reported above by the inclusive efficiency for this region. However, the result revealed a

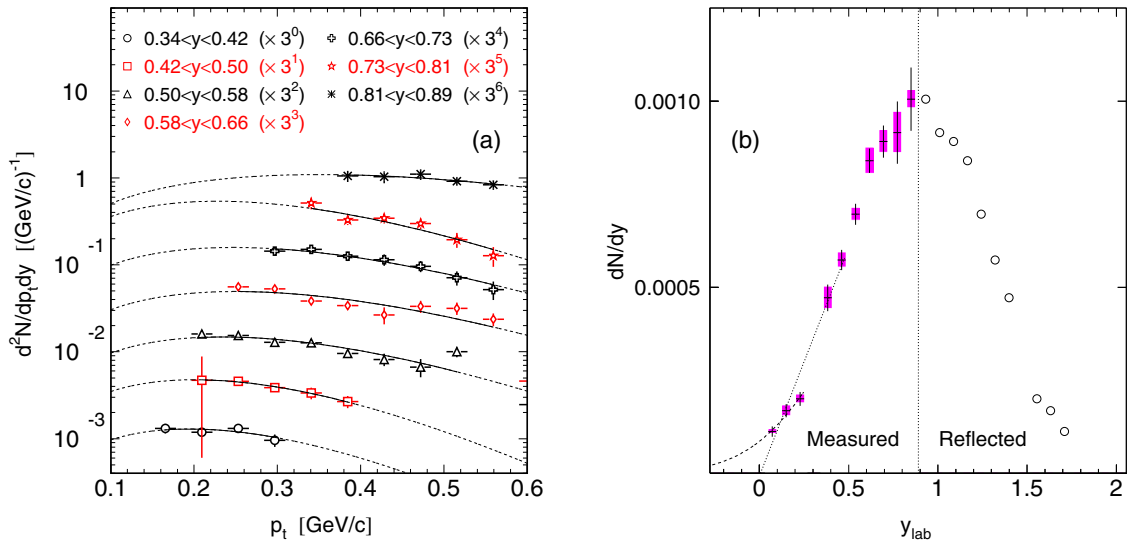

FIG. 4. (Color online) (a) Transverse momentum distributions of K^- for seven rapidity bins in the region $0.34 < y_{\rm lab} < 0.89$. Solid (dashed) curves denote the fitted (extrapolated) region. (b) Rapidity distribution of K^-. Data for $y_{\rm lab}$ above midrapidity (open circles) are the reflection of measured data points. Boxes indicate systematic errors of points within the selected binning. The dashed and dotted curves correspond to different extrapolation methods. The vertical line indicates the center of mass rapidity $y_{\rm NN}^{\rm CM} = 0.89$. See text for details.

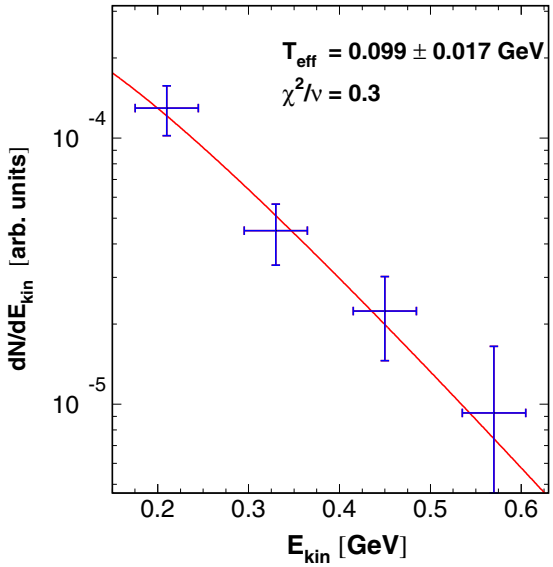

FIG. 5. (Color online) Kinetic energy distribution of ϕ mesons fitted with Boltzmann-like function, assuming the following input parameters to the efficiency calculation: $T_s = 100$ MeV, $\alpha = 0$ (see text for details).

clear correlation with the input temperature T_s of the source simulated in the efficiency evaluation procedure [cf. Eq. (1)]. It ranged between 3.2×10^{-4} for $T_s = 80$ MeV, and 6.2×10^{-4} for $T_s = 130$ MeV, not accounting for any statistical or systematic errors. This uncertainty was a motivation to study the kinetic energy spectrum of ϕ mesons, in the hope that, apart from carrying the kinematical information itself, it may provide constraints on the temperature, and thus limit the uncertainty of the total yield. The reconstructed kinetic energy spectrum, was fitted with the Boltzmann-like function of the form

$$\frac{dN}{dE_k} = NpE\exp(-E/T_{\rm eff}), \tag{6}$$

where N is the normalization parameter, total energy $E = E_k + m$, momentum $p = \sqrt{E^2 - m^2}$, and $T_{\rm eff}$ is called the inverse slope. An exemplary case of fitting the kinetic energy spectrum at $T_s = 100$ MeV, $\alpha = 0$, and events grouped in four bins, is shown in Fig. 5. The extracted value of $T_{\rm eff}$ was found to depend a little on a choice of binning of the E_k spectrum, T_s and α efficiency input parameters, particle identification cuts, and fit range imposed. However, only the fits obtained with the input T_s around the middle of the probed range of [80, 130] MeV resulted in values of $T_{\rm eff}$ fit parameter consistent with T_s. Following this finding, a self-consistency condition was imposed: $|T_s - T_{\rm eff}| < 15$ MeV, where 15 MeV is the typical statistical error of the fitted $T_{\rm eff}$. Note, that this condition not only narrows down the ranges of input T_s parameter, and the systematic error of $T_{\rm eff}$, but the selection of the T_s region also limits the systematic error of the total ϕ-meson yield discussed above. Within the imposed condition, the inverse slope of the kinetic energy distribution of ϕ mesons was found to be $T_{\rm eff} = 106 \pm 18({\rm stat})^{+18}_{-14}({\rm syst})$ MeV. The total yield was extracted by extrapolation of the data points with the fitted curve [Eq. (6)], and found to be

$$P(\phi) = [4.4 \pm 0.7({\rm stat})^{+1.6}_{-1.1}({\rm syst})] \times 10^{-4} \tag{7}$$

per triggered event, where the systematic errors are given at the 95% confidence level. We found, that the impact of nonzero anisotropy parameter α on the final results is on the level of 5% of this value.

C. Influence of ϕ production on K^- yields

The nearly 50% branching ratio of the $\phi \to K^+K^-$ decay channel, and the comparable yields of ϕ and K^- mesons suggest that their emission should be considerably correlated. However, while direct K^- are emitted from the hot collision zone, most decay products of ϕ mesons are created outside this region. Also, as the ϕ meson decays, a relatively small available energy is shared between two kaons, K^+ and K^-. Therefore, one may expect that negative kaons emitted from both these sources could have different kinematical characteristics. Hence, the question arises, what fraction of the observed K^- originate from the decays of ϕ mesons? For this analysis we find the following ratio of yields:

$$\frac{P(\phi)}{P(K^-)} = 0.44 \pm 0.07({\rm stat})^{+0.16}_{-0.10}({\rm syst}), \tag{8}$$

where the systematic errors were obtained by combining all the variations of both components due to their own systematic uncertainties, and rejecting 5% of values on the tails of the resulting distribution. Taking into account that 48.9% ϕ mesons decay into K^+K^- pairs, this translates into $22 \pm 4^{+8}_{-5}$% of observed K^- originating from decays of ϕ mesons. It is worthwhile noting that the same values within errors have been obtained for the Ar+KCl system colliding at even more subthreshold beam energy of 1.756A GeV [9]. Also, for the central Al + Al collisions at 1.9A GeV, a similar value of $P(\phi)/P(K^-) = 0.30 \pm 0.08({\rm stat})^{+0.04}_{-0.06}({\rm syst})$ was preliminarily reported [10,18]. However, for the elementary pp collisions at 2.7 GeV, this ratio was found to be slightly above 1 [19]. One possible explanation of this discrepancy arises in the context of the statistical model where the volume of open strangeness production is assumed to be limited and parametrized by the canonical radius R_C. According to the calculations reported in Ref. [9], the ϕ/K^- ratio measured for Ar+KCl is consistent with R_C between 2.2 and 3.2 fm, while that for pp is reproduced for $R_C \approx 1.2$ fm, although the latter prediction disagrees with the experimental data at higher beam energies. Unfortunately, performing the statistical model fit to the data was not possible for the present experiment, due to a meager amount of reconstructed particle yields available at centralities corresponding to $\langle A_{\rm part}\rangle_b \approx 50$. A much wider array of particle yields is available for the central collisions of the system in question (cf. Fig. 4(b) in Ref. [20]). A measurement of ϕ/K^- ratio for this centrality range would give an opportunity to extract the canonical radius parameter for the Ni+Ni system and compare with that for the Ar+KCl collisions.

In order to estimate the influence of ϕ mesons on the kinematic properties of the observed K^-, PLUTO code [21] was first employed to generate the thermal and isotropic ϕ mesons with temperature of 105 MeV, which subsequently decayed, giving rise to K^- production. The inverse slopes of

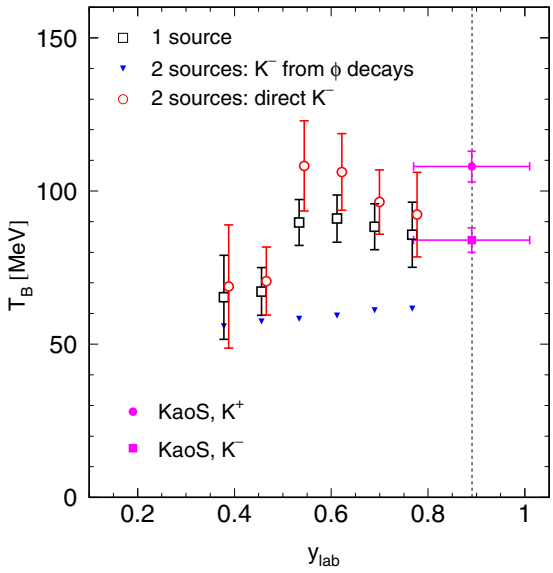

FIG. 6. (Color online) Rapidity distribution of T_B (apparent temperatures) for negative kaons within the one-source hypothesis (open squares), and two-source approach (K^- from ϕ decays: full triangles; direct kaons: open circles). Inverse slope of K^+ (K^-) obtained by the KaoS Collaboration is marked by full circle (square). See text for details.

the p_t spectra of such kaons, shown in Fig. 6 in full triangles, were found to be clearly lower than those of experimentally measured K^-, depicted with open squares. Following this finding, the emission of negative kaons was assumed to arise from two sources: the collision zone emitting kaons directly, and ϕ mesons decaying in vacuum. Their contributions were weighted according to the experimentally found ϕ/K^- ratio, and the phase-space distributions of both were assumed to be Boltzmann-like. For every slice of rapidity, the temperature parameter (inverse slope) of kaons from the ϕ-meson decays was fixed at a value obtained from the simulation described above, while the slope for the direct kaons was extracted by fitting the two-source model to the experimental data, giving the results shown in open circles in Fig. 6. Keeping in mind the limited statistics, and simplicity of the model, the results suggest that removing 22% contribution from ϕ mesons could systematically raise the inverse slope of K^- by up to about 15 MeV. It is worthwhile noting that similar conclusions were found in the collisions of Ar+KCl at the beam energy of 1.756A GeV [22].

In contrast, as the K^-/K^+ yield ratio is about 3% [6], the influence of ϕ mesons on positively charged kaons is negligible. The inverse slope parameters of the kinetic energy distributions of K^+ and K^-, obtained by the KaoS Collaboration at midrapidity for the same colliding system, and similar $\langle A_{\rm part}\rangle_b$, were found to exhibit a gap of about 25 MeV. Our finding suggests that the contribution from ϕ mesons to K^- emission significantly cools down the overall spectrum of negative kaons. Thus, this effect may account for a sizeable share of this gap, possibly competing with modifications of kaonic properties in the nuclear medium.

VI. SUMMARY

Production of ϕ and K^- mesons was investigated in Ni+Ni collisions at the beam kinetic energy of 1.91A GeV. The trigger selected a sample of central and semicentral collisions amounting to $(52.0 \pm 1.5)\%$ of the geometrical cross section. The p_t and $y_{\rm lab}$ distribution of K^- were analyzed in a wide region of phase space. The total yield of K^- was found to be $[9.84 \pm 0.21({\rm stat})^{+0.63}_{-0.57}({\rm syst})] \times 10^{-4}$ per triggered event. About 170 ϕ mesons were reconstructed. The inverse slope of kinetic energy distribution was found to be $T = 106 \pm 18({\rm stat})^{+18}_{-14}({\rm syst})$ MeV, and the total yield $[4.4 \pm 0.7({\rm stat})^{+1.6}_{-1.1}({\rm syst})] \times 10^{-4}$ per triggered event.

The found ϕ/K^- ratio of $0.44 \pm 0.07({\rm stat})^{+0.16}_{-0.10}({\rm syst})$ means that $22 \pm 4\,^{+8}_{-5}\%$ of K^- originate from decays of ϕ mesons, occurring mostly in vacuum. The influence of this additional source of negative kaons on the transverse momentum spectra was studied within a two-sources approach, where the contribution from ϕ-meson decays was modeled by an isotropic Boltzmann-like distribution. The inverse slopes of K^- produced directly in the collision zone seem to be up to about 15 MeV higher than the values extracted within the one-source hypothesis. This effect, compared to the 25 MeV gap between the inverse slopes of K^+ and K^-, signals that a considerable share of the gap could be explained by feeding of negative kaons by the ϕ-meson decays. Thus, it seems crucial to account for the contribution of ϕ-originating negative kaons in the studies of the in-medium modifications of these particles via comparisons of K^-/K^+ or flow (e.g., $v_{1,2}$) distributions to the predictions of the transport codes.

ACKNOWLEDGMENTS

This work was supported by the German BMBF PT-DESY Förderkennzeichen 05P12VHFC7, the Korea Science and Engineering Foundation (KOSEF) under Grant No. F01-2006-000-10035-0, by the German BMBF Contract No. 05P12RFFCQ, by the Polish Ministry of Science and Higher Education (DFG/34/2007), the agreement between GSI and IN2P3/CEA, the HIC for FAIR, the Hungarian OTKA Grant No. 71989, by NSFC (Project No. 11079025), by DAAD (PPP D/03/44611), by DFG (Projekt 446-KOR-113/76/04), and by the EU, 7th Framework Program, Integrated Infrastructure: Strongly Interacting Matter (Hadron Physics), Contract No. RII3-CT-2004-506078.

[1] C. Fuchs, Prog. Part. Nucl. Phys. **56**, 1 (2006).
[2] M. F. M. Lutz, Prog. Part. Nucl. Phys. **53**, 125 (2004).
[3] C. Hartnack, H. Oeschler, Y. Leifels, E. L. Bratkovskaya, and J. Aichelin, Phys. Rep. **510**, 119 (2012).
[4] B. Hong *et al.* (FOPI Collaboration), Phys. Lett. B **407**, 115 (1997).
[5] K. Wiśniewski *et al.* (FOPI Collaboration), Eur. Phys. J. A **9**, 515 (2000).

[6] A. Förster *et al.* (KaoS Collaboration), Phys. Rev. C **75**, 024906 (2007).
[7] X. Lopez *et al.* (FOPI Collaboration), Phys. Rev. C **76**, 052203(R) (2007).
[8] A. Mangiarotti *et al.* (FOPI Collaboration), Nucl. Phys. A **714**, 89 (2003).
[9] G. Agakishiev *et al.* (HADES Collaboration), Phys. Rev. C **80**, 025209 (2009).
[10] P. Gasik, K. Wiśniewski, and T. Matulewicz, Acta Phys. Pol. B **41**, 379 (2010).
[11] B. B. Back *et al.* (E917 Collaboration), Phys. Rev. C **69**, 054901 (2004).
[12] H. W. Barz, M. Zétényi, Gy. Wolf, and B. Kämpfer, Nucl. Phys. A **705**, 223 (2002).
[13] M. Kiš *et al.* (FOPI Collaboration), Nucl. Instr. Meth. A **646**, 27 (2011).
[14] J. Ritman, Nucl. Phys. (Proc. Suppl.) B **44**, 708 (1995); B. Sikora, Acta Phys. Pol. B **31**, 135 (2000).
[15] Particle Data Group, K. A. Olive *et al.*, Chin. Phys. C **38**, 090001 (2014).
[16] wwwasdoc.web.cern.ch/wwwasdoc/geant_html3/geantall.html
[17] C. Hartnack *et al.*, Eur. Phys. J. A **1**, 151 (1998).
[18] P. Gasik, Ph.D. thesis, University of Warsaw, 2011.
[19] Y. Maeda *et al.*, Phys. Rev. C **77**, 015204 (2008).
[20] K. Piasecki, Acta Phys. Pol. B **41**, 405 (2010).
[21] I. Frohlich *et al.*, PoS **ACAT2007**, 076 (2007).
[22] M. Lorenz (HADES Collaboration), PoS (BORMIO2010) **038**, 1 (2010).